



# Optic Flow Based Visual Guidance: From Flying Insects to Miniature Aerial Vehicles

Nicolas Franceschini, Franck Ruffier, Julien Serres, Stéphane Viollet

## ► To cite this version:

Nicolas Franceschini, Franck Ruffier, Julien Serres, Stéphane Viollet. Optic Flow Based Visual Guidance: From Flying Insects to Miniature Aerial Vehicles. *Aerial Vehicles*, InTech, 2009, 10.5772/6491 . hal-03042183

HAL Id: hal-03042183

<https://amu.hal.science/hal-03042183>

Submitted on 6 Dec 2020

**HAL** is a multi-disciplinary open access archive for the deposit and dissemination of scientific research documents, whether they are published or not. The documents may come from teaching and research institutions in France or abroad, or from public or private research centers.

L'archive ouverte pluridisciplinaire **HAL**, est destinée au dépôt et à la diffusion de documents scientifiques de niveau recherche, publiés ou non, émanant des établissements d'enseignement et de recherche français ou étrangers, des laboratoires publics ou privés.

# Optic Flow Based Visual Guidance: From Flying Insects to Miniature Aerial Vehicles

Nicolas Franceschini, Franck Ruffier, Julien Serres and Stéphane Viollet  
*Biorobotics Lab, Institute of Movement Science, CNRS & Aix-Marseille University  
 France*

## 1. Introduction

Insects and birds have been in the sensory-motor control business for more than 100 million years. The manned aircraft developed over the last 100 years rely on a similar lift to that generated by birds' wings. Aircraft designers have paid little attention, however, to the pilot's *visual sensor* that finely controls these wings, although it is definitely the most sophisticated avionic sensors ever known to exist. For this reason, the thinking that prevails in the field of aeronautics does not help us much grasp the visuo-motor control laws that animals and humans bring into play to control their flight. To control an aircraft, it has been deemed essential to measure state variables such as barometric altitude, groundheight, groundspeed, descent speed, etc. Yet the sensors developed for this purpose - usually emissive sensors such as Doppler radars, radar-altimeters or forward-looking infrared sensors, in particular - are far too cumbersome for insects or even birds to carry and to power. Natural flyers must therefore have developed other systems for controlling their flight.

Flying insects are agile creatures that navigate swiftly through most unpredictable environments. Equipped with "only" about one million neurons and only 3000 pixels in each eye, the housefly, for example, achieves 3D navigation at an impressive 700 body-lengths per second. The lightness of the processing system at work onboard a fly makes us turn pale when we realize that this creature actually achieves just what is being sought for in the field of aerial robotics: dynamic stabilization, 3D autonomous navigation, ground avoidance, collision avoidance with stationary and nonstationary obstacles, tracking, docking, autonomous takeoff and landing, etc. Houseflies add insult to injury by being able to land gracefully on ceilings.

The last seven decades have provided evidence that flying insects guide themselves through their environments by processing the *optic flow* (OF) that is generated on their eyes as a consequence of their locomotion. In the animal's reference frame, the translational OF is the *angular speed*  $\omega$  at which contrasting objects in the environment move past the animal (Kennedy, 1939; Gibson, 1950; Lee, 1980; Koenderink, 1986).

In the present chapter, it is proposed to summarize our attempts to model the visuomotor control system that provides *flying* insects with a means of autonomous guidance at close range. The aim of these studies was not (yet) to produce a detailed neural circuit but rather to obtain a more functional overall picture, that is, a picture that abstracts some basic control

principles (Marr, 1982). We attempted to determine the variables the insect really measures (see also: Taylor & Krapp, 2008), the actions it takes to control its flight and the causal and dynamic relationships between the sensory and motor variables involved.

Our progress on these lines was achieved by performing simulation experiments and testing our control schemes onboard miniature aircraft. Like our early terrestrial "robot-mouche" (robot Fly) (Pichon et al., 1989; Franceschini et al., 1992), these aerial robots are based on the use of an electronic *OF sensor* (Blanes, 1986) inspired by the housefly Elementary Motion Detectors (EMD), which we previously studied in our laboratory (Rev.: Franceschini, 1985; Franceschini et al., 1989).



Figure 1. Head of the blowfly *Calliphora erythrocephala* with its panoramic compound eyes (left). The right part shows about 2% of the housefly retinal mosaic. A cluster of micrometer-sized photoreceptors is located in the focal plane of each facet lens : 6 outer receptors R1-6 surround a central cell R7 (prolonged by an R8, not seen here). These are the natural *autofluorescence* colors of the receptors observed *in vivo* under blue excitation (Franceschini et al., 1981a,b), after « optical neutralization of the cornea » (From Franceschini, 2007)

Section 2 recalls some aspects of the fly visual system. Section 3 focuses on the realisation of fly-inspired OF sensors. Section 4 examines the problem of ground avoidance. Section 5 introduces the *OF regulator*. In Section 6 the miniature helicopter we built is described, equipped with an electronic *OF sensor* and an *OF regulator*. The extent to which the *OF regulator* accounts for the actual behavioral patterns observed in insects is discussed in Section 7. Section 8 introduces the *dual OF regulator* that is able to control both speed and distance to the walls in a corridor. In Section 9, another visuomotor control system is presented which enables an aerial robot to stabilize in yaw by visually fixating a target with *hyperacuity*, on the basis of a principle inspired by the fly. Section 10 ends up by discussing the potential applications of these insect-derived principles to the navigation of aerial vehicles - in particular Micro Aerial Vehicles (MAVs) and Micro Space Vehicles (MSVs).

## 2. The fly visual system and its motion sensitive neurons

Each compound eye consists of an array of *ommatidia*, the frontend of which is a facet lens that focusses light on a small group of photoreceptor cells (Fig. 1, right). The fly retina is among the most complex and best organized retinal mosaic in the animal kingdom. It has been described in great details, with its different spectral types of photoreceptor cells, polarization sensitive cells and sexually dimorphic cells. There exists a typical *division of labour* within the retina (Rev.: Franceschini, 1984; Hardie, 1985):

- The two central photoreceptor cells, R7-8, display various spectral sensitivities that are randomly scattered across the retinal mosaic, as attested by the characteristic R7 autofluorescence colors (Fig. 1). R7 and R8 are thought to participate in *color vision*.
- The outer 6 photoreceptor cells (R1-R6) all have the same, wide-band spectral sensitivity. They participate, in particular, in *motion detection* (Rev.: Buchner, 1984, Heisenberg & Wolf, 1984; Riehle & Franceschini, 1984). In this visual pathway, signal-to-noise ratio is improved by the presence of an ultraviolet sensitizing pigment that enhances their quantum catch (Kirschfeld & al., 1977), and by an exquisite opto-neural projection called "*neural superposition*" (Braitenberg, 1967; Kirschfeld, 1967; Kirschfeld and Franceschini, 1968). The R1-R6 photoreceptors therefore make for a high sensitivity ("scotopic") system (Kirschfeld and Franceschini, 1968).

To estimate the OF, insects use motion sensitive neurons. In flies, part of the 3rd optic ganglion called the *Lobula Plate* (LP) appears as a genuine "visual motion processing center". It comprises approximately 60 *uniquely identifiable* neurons, the LP tangential cells (LPTC) that analyze the OF field resulting from the animal's walking or flying. Some of these neurons transmit their electrical signals via the neck to thoracic interneurons that will drive the wing-, leg-, and head-muscles. Other neurons (in particular H1, see Fig. 2b) send their signals to the contralateral eye. The LPTCs are actually large-field collator neurons that pool the electrical signals from many retinotopic input elements called 'Elementary Motion Detectors' (EMDs) (Rev.: Hausen & Egelhaaf, 1989; Egelhaaf & Borst, 1993; Hausen, 1993; Krapp et al., 1998; Borst & Haag, 2002, Taylor & Krapp, 2008). The cellular details underlying an EMD has not been fully identified in any insects - nor in any vertebrates.

Taking advantage of the micro-optical techniques we had developed earlier (Rev.: Franceschini, 1975), we were able, however, to activate a single EMD in the eye of the living housefly by stimulating single *identified* photoreceptor cells within a single ommatidium while recording the response of an *identified* motion sensitive neuron (H1) in the LP (Riehle & Franceschini, 1984, Franceschini, 1985, 1992; Franceschini et al., 1989). We applied pinpoint stimulation to two neighboring photoreceptors (diameter  $\approx 1\mu\text{m}$ ) within the selected ommatidium (Fig. 2a) by means of an optical stimulation instrument (Fig. 2d) whose main objective was quite simply the facet lens itself (diameter  $\approx 25 \mu\text{m}$ , focal length  $\approx 50 \mu\text{m}$ ). This exact instrument (a rotating triple beam incident light 'microscope-telescope') served to : (i) select a facet lens, (ii) select 2 out of the 7 receptors (R1 and R6), and (iii) stimulate them *successively* with  $1\mu\text{m}$ -light spots. Sequential stimulation produced an 'apparent motion' that would *simulate* a real motion within the small visual field of the selected ommatidium. The H1-neuron responded by a conspicuous *increase* in spike rate, as long as the phase relationship between the two stimuli mimicked a movement occurring in the *preferred* direction (see Fig. 2c, top trace). The null response observed for the reverse sequence (Fig 2c, bottom trace) attests to the remarkable sequence discriminating ability of an EMD, which is sensitive to *directional motion* (Franceschini, 1992).

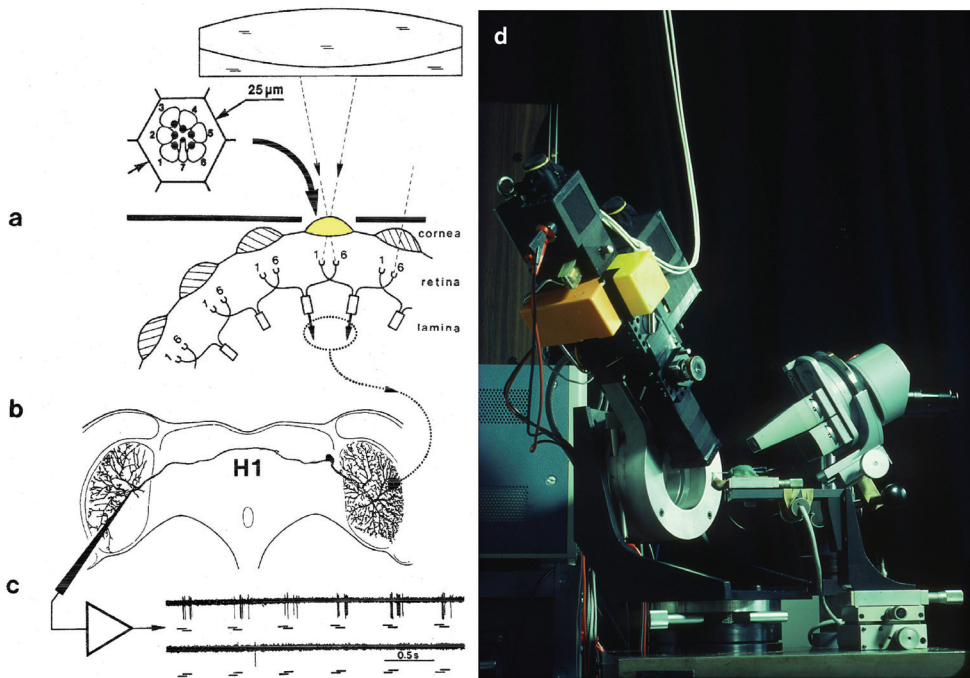


Figure 2. (left) : (a-c) Principle of the experiment aimed at deciphering the principle of motion vision in flies, using optical stimulation of single photoreceptors. (d) Triple-beam incident light "microscope-telescope" that delivers a 1mm light spot to two neighboring photoreceptor cells, R1 and R6, successively (see (a)). A microelectrode (c) records the electrical response (nerve impulses) of the motion sensitive neuron H1 to this "apparent motion" (From Franceschini et al., 1989)

From many experiments of this kind, in which various sequences of light steps and/or pulses were applied to selected receptor pairs, we established an EMD *block diagram* and characterized each block's dynamics and nonlinearity (Franceschini, 1985, 1992; Franceschini et al., 1989). While not unveiling the cellular details of the EMD circuit, our analysis allowed the EMD principle to be understood *functionally*, paving the way for its transcription into another, man-made technology.

### 3. From biological to electronic optic flow sensors

In the mid 1980's, we designed a neuromorphic optic flow sensor (Blanes, 1986, 1991, Franceschini et al., 1986), the signal processing scheme of which was inspired by what we had learned from the fly EMD. The OF is an angular speed  $\omega$  that corresponds to the inverse of the time  $\Delta t$  taken by a contrasting feature to travel between the visual axes of two adjacent photoreceptors, separated by an angle  $\Delta\phi$ . Our OF sensor processes this delay  $\Delta t$  so as to generate a response that grows monotonically with the inverse of  $\Delta t$ , and hence with the optic flow  $\omega$  (Fig. 3a). Short delays  $\Delta t$  give higher voltage outputs and vice versa.

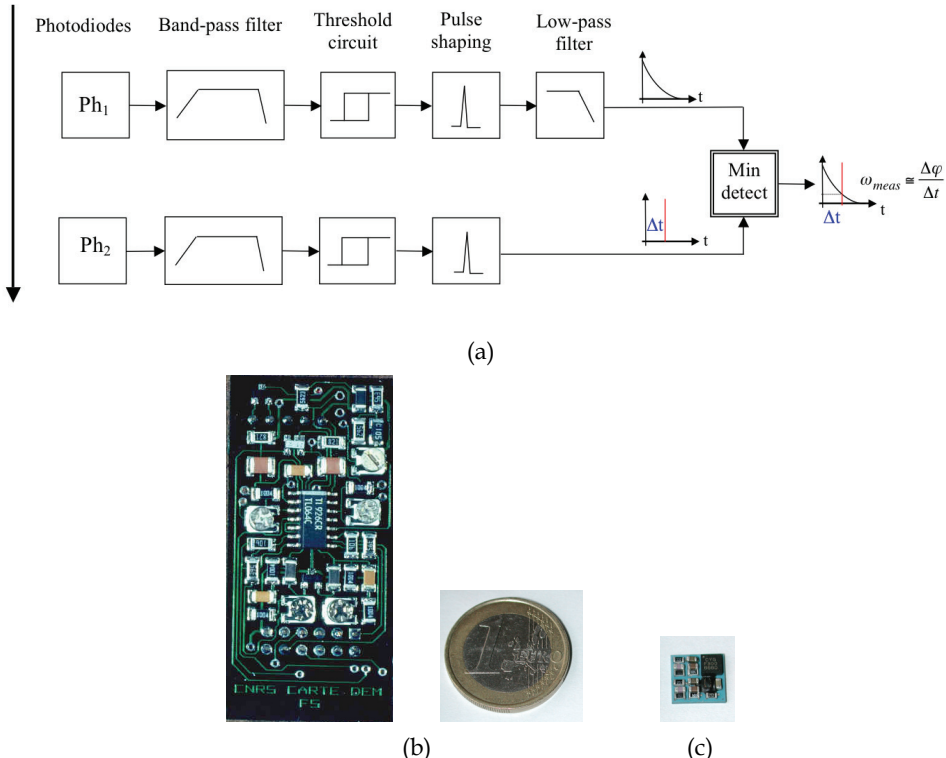


Figure 3. (a) Principle of the optic flow sensor derived from our electrophysiological analyses of the housefly's EMD (Blanes, 1986, Franceschini et al., 1986). (b) purely analogue version (weight 5 grams) built in 1989 for robot Fly, whose compound eye housed a ring of 114 EMDs of this type (Pichon et al., 1989 ; Blanes, 1991 ; Franceschini & al., 1992) (c) hybrid (analogue + digital) version (size : 7mm x 7 mm, mass 0.2 grams) based on a microcontroller and built using Low Temperature Co-fired Ceramics technology (LTCC) (Pudas et al., 2007)

Our scheme is not a “correlator scheme” (cf Hassenstein & Reichardt, 1956, Reichardt, 1969) and corresponds to the class of “feature-matching schemes” (Ullman, 1981), where a given feature (here a change in intensity that may represent an edge) is extracted and tracked in time. The photodiode signal of each channel is first *bandpass filtered* (Fig. 3a) - resembling the analog signal measured in the large monopolar neurons of the fly lamina (Laughlin, 1984). The next step consists of hysteresis thresholding and generation of a unit pulse. In the EMD version built in 1989 for robot Fly (Fig. 3b), the unit pulse from one channel was sampling a long-lived decaying exponential function generated by the other channel (Blanes, 1991), via a nonlinear circuit called a minimum detector, to give an output  $\omega_{measured}$  that grows as a monotonic function of the angular velocity  $\omega = \Delta\varphi/\Delta t$  (Fig. 3). The thresholding operation makes the voltage output virtually independent of texture and contrast – unlike the Reichardt correlator – and the circuit responds as well to natural scenes (Portelli et al., 2008). A very similar EMD principle has been conceived, independently, a decade later by C. Koch’s group at CALTECH, where it became

known as the “facilitate and sample” velocity sensor (Kramer et al., 1995). Yet another variant of our original “time of travel” principle was proposed another decade later (Möckel & Liu, 2006). Since our original analog design (Blanes, 1986, 1991; Franceschini et al., 1986) we have built various versions of OF sensors based on this very principle. In the EMD currently used onboard our aerial robots, the signals are processed using a mixed (analog + digital) approach (Ruffier et al., 2003). Such OF sensors can be small and lightweight (the smallest one weighs only 0.2 grams: Fig. 3c) to mount onto MAVs. Several OF sensors of this type were also recently integrated on a miniature FPGA (Aubépart et al. 2004, 2008; Aubépart & Franceschini, 2007). A different kind of OF sensor was designed recently (Barrows et al., 2001) and mounted on a model plane (Barrows et al., 2003; Green & Barrows, 2004).

#### 4. The problem of ground avoidance

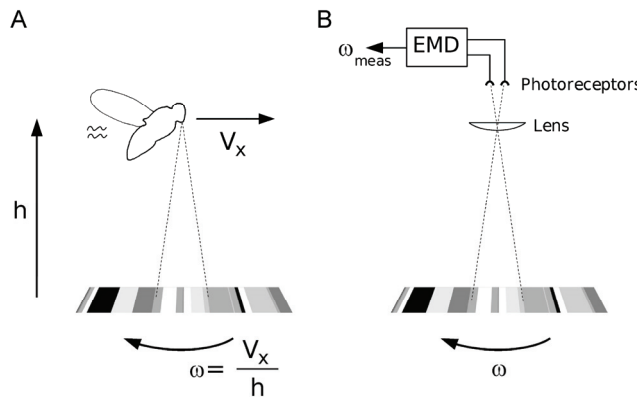


Figure 4. Definition (a) and measurement of the ventral optic flow  $\omega$  experienced by an insect (or a robot) flying in translation in the vertical plane. (b) an EMD of the type shown in Fig. 3, like the EMDs driving the honeybees' VT neurons (Ibbotson, 2001), is able to measure the ventral OF, i.e., the angular speed  $\omega$  at which a contrasting feature moves under the flying agent (From Franceschini et al., 2007)

The ventral OF experienced in the vertical plane by flying creatures - including aircraft pilots - is the apparent *angular velocity*  $\omega$  generated by a point directly below on the flight track (Gibson et al., 1955; Whiteside & Samuel, 1970). As shown in figure 4a, the ventral OF depends on both the groundspeed  $V_x$  and the groundheight  $h$  and is equal to the ratio between these two variables:

$$\omega = V_x / h \text{ [rad.s}^{-1}\text{]} \quad (1)$$

We know that flies and bees are able to react to the *translational OF* independently of the spatial texture and contrast (David, 1982; Kirchner & Srinivasan, 1989; Srinivasan et al., 1991, 1993; Baird et al., 2005). We also know that some of their visual neurons may be involved in this reaction because they respond monotonically to  $\omega$  with little dependence on texture and contrast (Ibbotson, 2001; Shoemaker et al., 2005; Straw et al., 2008). Neurons facing downwards can therefore act as ventral OF sensors, and thus assess the  $V_x/h$  ratio (figure 4). Based on laboratory experiments on mosquitoes and field experiments on locusts, Kennedy put forward an “optomotor theory” of insect flight, according to which flying insects

maintain a “preferred retinal velocity” with respect to the ground below (Kennedy, 1939, 1951). In response to wind, for example, insects may adjust their groundspeed or groundheight to restore the apparent velocity of the ground features. Kennedy’s hypothesis has been repeatedly confirmed during the last 30 years: both flies and bees were found to maintain a constant OF with respect to the ground while cruising or landing (David, 1978; Preiss, 1992; Srinivasan et al., 1996, 2000, Baird et al., 2006).

The problem is *how* insects may achieve this feat, since maintaining a given OF is a kind of chicken-and-egg problem, as illustrated by Eq.1: an insect may hold its ventral OF,  $\omega$ , constant by adjusting either its groundspeed (if it knows its groundheight) or its groundheight (if it knows its groundspeed). Besides, the insect could maintain an OF of 1rad/s (i.e., 57°/s), for instance, by flying at a speed of 1m/s at a height of 1 meter or by flying at a speed of 2m/s at a height of 2m: there is an infinitely large number of possible combinations of groundspeed and groundheight that will give rise to the same “preferred OF”.

Drawing on the experience we had with OF-based visual navigation of a terrestrial robot (Pichon et al., 1989; Franceschini et al., 1992), we attempted early to develop an explicit flight control scheme for aerial navigation in the vertical plane. Our first tentative step on these lines was not particularly successful, because we were cornered in the general notion that prevailed in those days that insect navigation relies on *gauging range* (Kirchner & Srinivasan, 1989; Srinivasan et al., 1991; Franceschini et al., 1992; Srinivasan, 1993). In the experimental simulations we performed in 1994, for example (Mura & Franceschini, 1994), we assumed that the insect (or the robot) would know its groundspeed  $V_x$  (by whatever means), so that by measuring  $\omega$  it would be able to gauge the distance  $h$  from the ground (Eq.1) and react accordingly to avoid it. Although this procedure may be justified in robotics (see, e.g., Barber et al, 2005; Srinivasan, 2006; Garratt & Chahl, 2008), where groundspeed can be determined via GPS, this makes the way insects operate all the more elusive.

In 1999, we established (in simulation) *how* a rotorcraft (or an insect) might be able follow a terrain (Fig. 5a) and land (Fig. 5b) on the sole basis of OF cues, *without measuring its groundspeed and groundheight* (Netter & Franceschini, 1999).

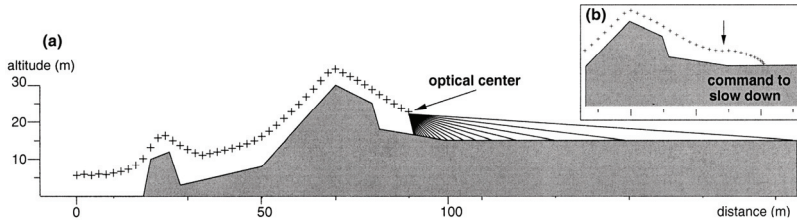


Figure 5. (a) Simulation of nap-of-the-earth flight of an helicopter equipped with an eye whose 20 pixels cover a frontal FOV of 75° in the vertical plane, centered at 40° below the horizon (initial conditions: height: 5m, speed 2m/s; iteration step 1s). (b) Landing was initiated by linearly decreasing the aircraft horizontal speed at every iteration while retaining the same request to maintain a reference OF value (From Netter & Franceschini, 1999)

The landing manoeuvre was achieved under permanent visual feedback from a 20-pixel forward looking eye (with 19 EMDs). The driving force causing the progressive loss in altitude was the decrease in the horizontal flight speed, which occurred when the rotorcraft (or the insect) decreased its speed to land - either voluntarily or in the presence of a headwind. The landing trajectory obtained in this simulation (Fig. 5b) already resembles the final approach of

bees landing on a smooth surface (Srinivasan et al, 1996). The principle was first validated onboard FANIA, a miniature tethered helicopter having a single (variable pitch) rotor, an accelerometer and a forward looking eye with 20 pixels (and, therefore, 19 EMDs) arranged in the frontal meridian (Netter & Franceschini, 2002). This 0.8-kg rotorcraft had three degrees of freedom (surge, heave and pitch). Mounted at the tip of a flight mill, the robot lifted itself by increasing its rotor collective pitch. Upon remotely inclining the servo-vane located in the propeller wake, the operator made the helicopter pitch forward by a few degrees so that it gained speed and, therefore, climbed to maintain a reference OF with respect to the terrain below. FANIA jumped over contrasting obstacles by increasing its collective pitch as a function of the fused signals from its 19 EMDs (see Fig. 8 in Netter & Franceschini, 2002).

## 5. The “optic flow regulator”

In spite of this early success to explain how an insect could navigate on an OF basis, we considered that Kennedy’s insightful “optomotor theory” was calling for a clear formalization that would bring to light:

- the flight variables really involved
- the sensors really required
- the dynamics of the various system components
- the causal and dynamic links existing between the sensory output(s) and the variable(s) to be controlled
- the point of application of the various disturbances that an insect will experience in flight and the variables it will have to control to compensate for these disturbances.

We came up with an autopilot called OCTAVE (OCTAVE stands for Optical altitude Control sysTem for Autonomous VEhicles) that is little demanding in terms of neural (or electronic) implementation and could be just as appropriate for insects as it would be for aircraft (Ruffier & Franceschini, 2003). A ventral OF sensor was integrated into a feedback loop that would drive the robot’s lift, and thus the groundheight, so as to compensate for any deviations of the OF sensor’s output from a given set point (Ruffier & Franceschini, 2003, 2004a,b, 2005; Franceschini et al., 2007). This simple autopilot (Fig. 6a) enabled a miniature helicopter to perform challenging tasks such as take-off, terrain following, reacting suitably to wind, and landing (see Section 6).

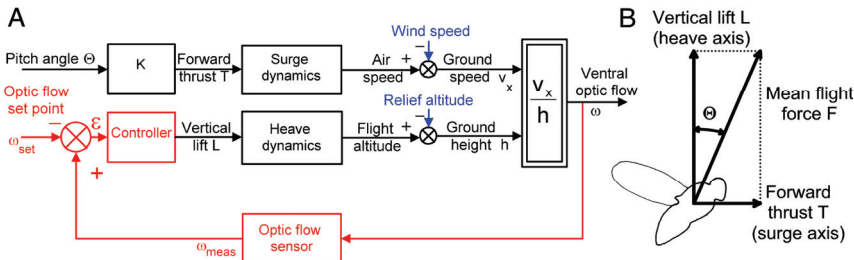


Figure 6. (a) The OF regulator OCTAVE (bottom red feedback loop) controls the lift  $L$ , and consequently the groundheight, at all times so as to maintain the ventral optic flow  $\omega$  constant and equal to the set-point  $\omega_{set}$ . (b) Flies and bees, like helicopters, pitch forward to increase their forward thrust, and hence their airspeed. As long as they pitch forward by  $\Theta < 10^\circ$ , the lift component  $L$  does not incur any major loss (From Franceschini et al., 2007)

The OCTAVE autopilot can be said to be an *OF regulator*. The word ‘regulator’ is used here in the strictest acceptance of the word in the context of control theory, where it describes a *feedback control system* designed to maintain an output signal constantly equal to a given set point. The Watt flyball governor from the 18<sup>th</sup> century, for instance, was not only one of the first servomechanisms ever built: it was also the very first *angular speed regulator*. It served to maintain the rotational speed of a steam engine shaft at a given set point, whatever interferences occurred as the result of unpredictable load disturbances. The Watt regulator was based on a rotational speed sensor (meshed to the output shaft), whereas our *OF regulator* was based on a noncontact rotational speed sensor - the *OF sensor* - that measures the ventral OF - again in rad/s.

Specifically, the OF signal  $\omega_{meas}$  delivered by the OF sensor (see Fig. 6a) is compared with the OF set-point,  $\omega_{set}$ . The comparator produces an error signal:  $\epsilon = \omega_{meas} - \omega_{set}$  which drives a controller adjusting the lift  $L$ , and thus the groundheight  $h$ , so as to minimize  $\epsilon$ . All the operator does is to set the pitch angle  $\Theta$  and therefore the airspeed (see figure 6a): the *OF regulator* does the rest, that is, it adjusts the groundheight  $h$  proportionally to the current groundspeed  $V_x$ , keeping the OF, i.e., the  $V_x/h$  ratio constant in the steady state:

$$V_x/h = \omega \approx \omega_{meas} \approx \omega_{set} = \text{constant} \quad (2)$$

Upon looking at figure 6b, one might be tempted to object that controlling  $F$  (via the rotor speed) will affect not only  $L$  but also  $T$ . This *coupling* is negligible, however, because the ensuing change in  $T$  is *much smaller* than the change in  $L$  (by a factor of at least  $5.67 = \cotan 10^\circ$ , because the maximum speed of 3m/s is already attained for  $\Theta = 10^\circ$ ).

## 6. A miniature helicopter equipped with an “optic flow regulator”

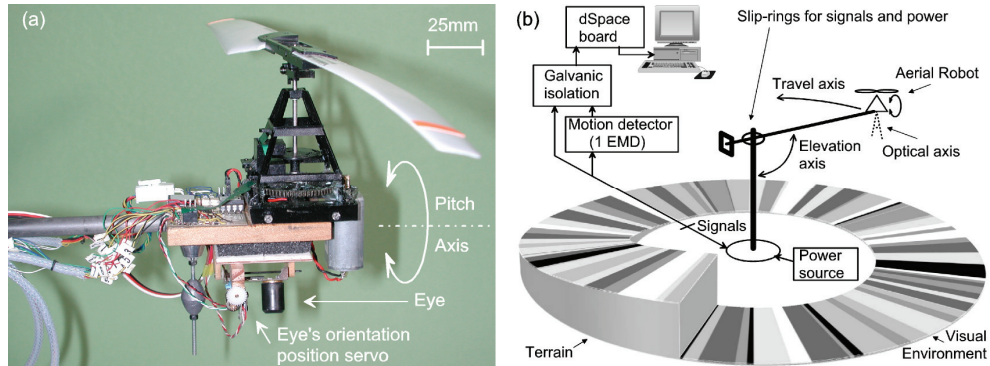


Figure 7. (a) Miniature helicopter (MH) equipped with an *OF sensor* and an *OF regulator* (Fig. 6). The operator sets the forward pitch, and thus the airspeed. The gaze remains automatically oriented downwards. (b) The 100-gram robot lifts itself and circles around CCW at speeds up to 3m/s and heights up to 3 m over the arena, giving rise to the flight patterns given in Fig. 8-10 (From Ruffier & Franceschini, 2003, 2004b)

We tested the idea that insects may be equipped with a similar *OF regulator* by comparing the behavior of insects with that of a ‘seeing helicopter’ placed in similar situations. The robot we built (figure 7a) is a miniature helicopter (MH) equipped with a simple, 2-pixel ventral eye driving an EMD acting as an OF sensor (Fig. 6). The 100-gram robot is tethered

to an instrumented flight mill consisting of a light pantographic arm driven in terms of its elevation and azimuth by the MH's lift and forward thrust, respectively (Fig. 7b).

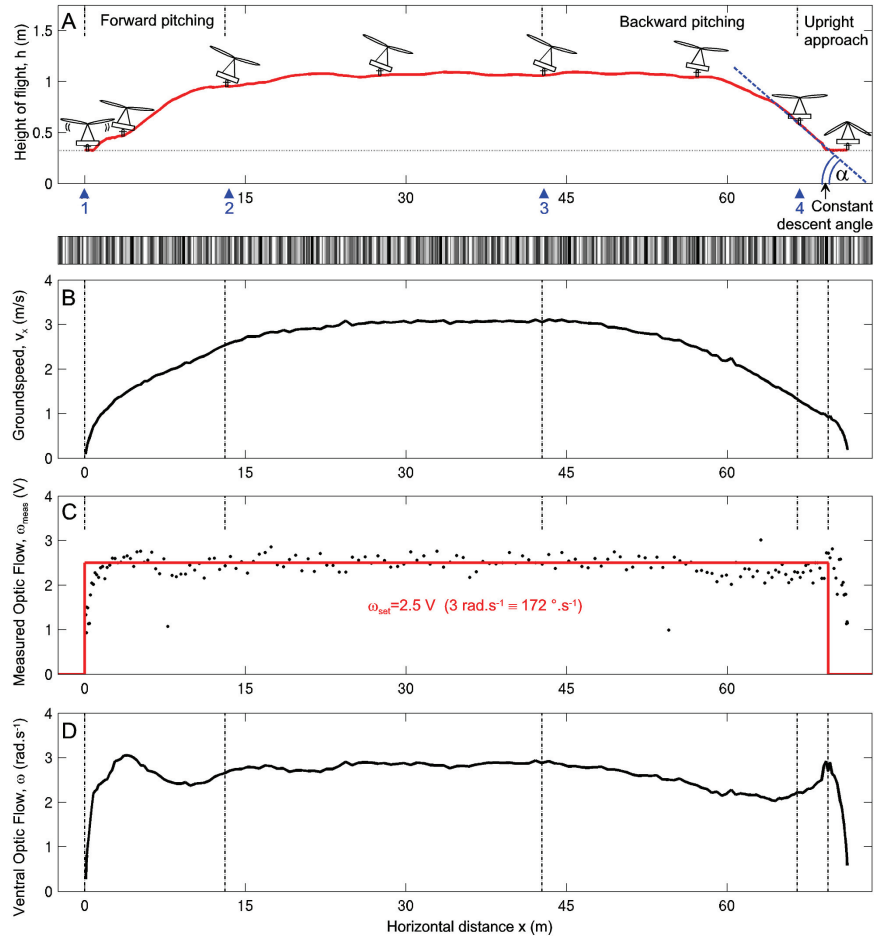


Figure 8. Flight parameters monitored during a 70-meter flight (consisting of about 6 laps on the test arena: figure 7b) performed by the miniature helicopter (MH) (Fig. 7a), equipped with an OF regulator (figure 6a). The complete journey over the randomly textured pattern (shown at the bottom of (a)) includes take-off, level flight and landing

(a) Vertical trajectory in the longitudinal plane. (b) Groundspeed  $V_x$  monitored throughout the journey. (c) Output  $\omega_{\text{neas}}$  of the OF sensor showing the relatively small deviation from the OF set point  $\omega_{\text{set}}$  (red curve). (d) Actual OF,  $\omega$  (calculated as  $V_x/h$ ) resulting from the behavioral reaction:  $\omega$  is seen to have been held relatively - but not perfectly - constant throughout the journey, even during the takeoff and landing maneuvers where the groundspeed varies considerably (From Franceschini et al., 2007).

Any increase in the rotor speed causes the MH to rise, and the slightest (operator mediated) forward ("nose-down") tilting by a few degrees produces a forward thrust component that causes the MH to gain forward speed. The flight mill is equipped with ground-truth azimuthal and elevation sensors that allow the position and speed of the MH to be monitored at high accuracy and in real time. Since the MH purpose was to demonstrate a basic principle, it was equipped with an elementary ventral eye composed of only two photoreceptors driving a single Elementary Motion Detector (EMD) built according to the principle shown in Fig. 3 (Ruffier & Franceschini, 2003, Ruffier et al., 2003).

## 7. Comparison of robots' and insects' behavioral patterns

The OCTAVE control scheme (Fig. 6) produced the helicopter behavioral patterns shown in figures 8-10. The robot's behavior was found to account for a series of puzzling, seemingly unconnected flying abilities observed by many authors during the last 70 years in various species (fruitflies, honeybees, moths, mosquitoes, dung-beetles, migrating locusts and butterflies, and birds) (Franceschini et al., 2007). Most of the data published in these studies are qualitative, but recent quantitative findings on honeybees' landing performances can also be explained on the basis of this simple control scheme, including the constant descent angle observed in the bee's final approach (Srinivasan et al., 1996, 2000).

Let us now examine these various behavioral patterns, assuming the insect to be equipped with the *OF regulator* shown in Fig. 6 (Franceschini et al., 2007).

### 7.1 Take-off

An insect that increases its forward thrust by pitching forward (Fig. 6b) like a fly (David, 1978) or a helicopter, is bound to rise into the air because the OF regulator (Fig. 6a) will constantly increase the groundheight  $h$  proportionally to the current groundspeed  $V_x$ , to maintain the OF constant (Eq.2).

The performances of the MH illustrate this point quite clearly (figure 8a, left part). Starting at position 1 (with the rotor axis oriented vertically and the lift just balancing the weight), the MH is remotely commanded to pitch 'nose-down' ( $\Theta$  from  $0^\circ$  to  $+10^\circ$  rampwise). The ensuing increase in groundspeed (figure 8b) automatically causes the micro-flyer to rise (figure 8a) because the feedback loop slaves  $h$  to  $V_x$ , effectively maintaining the actual ratio  $\omega = V_x/h$  relatively constant throughout take-off (figure 8d). Upon reaching a steady groundspeed of  $3 \text{ m.s}^{-1}$  (Figure 8b), the MH can be seen to have cruised at a steady groundheight (of around one meter: figure 8a), which depends on the OF set-point (here,  $\omega_{set} = 3 \text{ rad.s}^{-1}$ : figure 8c).

### 7.2 Terrain following

An increase in relief absolute altitude constitutes a "disturbance" that causes a reduction in the local groundheight  $h$ . This disturbance will be compensated for by an increase in flight altitude (see figure 6a). Figure 9a shows that the MH is able to clear a gentle slope. Figure 9b confirms the prediction made at the end of Section 5 that the groundspeed hardly changes in spite of the changes in the mean flight force  $F$  needed to change the altitude (see figure 6b). Insects are able to follow a terrain or a canopy and the above scheme may explains how they achieve this feat. Migrating butterflies crossing narrow canyons fly down into the gully and across the bottom. When traversing dense forests, they clear the canopy at a distance

roughly equal to their previous height above the ground, and once they have crossed this large obstacle, they re-descend (Srygley & Oliveira, 2001).

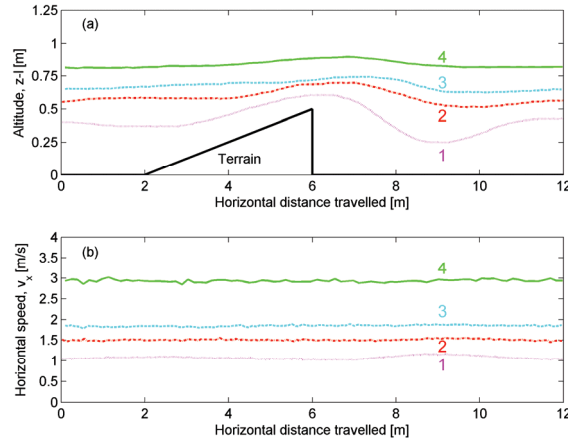


Figure 9. Terrain following by the miniature helicopter (Fig. 7a) recorded at 4 different groundspeeds (1m/s ; 1.5 m/s; 1.8 m/s; 3 m/s). The altitude  $z-l$  plotted in (a) is that of the landing gear which is at a distance  $l= 0.3$  m under the eye. The higher the speed, the higher the clearance from the terrain (From Ruffier & Franceschini, 2003)

Figure 9 shows that when the MH is set to travel at a higher speed, it automatically maintains a greater height above the terrain, giving rise to a "safe" flight. This is precisely the flight pattern that was observed in dung-beetles: they fly higher at higher groundspeeds and lower at lower speeds (Steiner, 1953). Likewise, bees cruise at a height roughly proportional to their horizontal flight speed (see Fig. 7c in Srinivasan et al., 2000). In other words, there is a similarly tight link between groundspeed and groundheight in insects and our helicopter. What the explicit control scheme (Fig. 6) brings to the fore is a specific causal link: it is the change in groundspeed that induces the change in groundheight, and not the other way round (this point is discussed further in Section 8).

### 7.3 Flying against wind

Locusts and other migrating insects have long been known to descend under headwind and ascend during lull (Kennedy, 1951, Srygley & Olivera, 2001). Under headwind conditions, Braüniger (1964) observed that bees were flying at such a low speed and so close to the ground that he was able to accompany them on his bicycle all the way to the nectar source. Windspeed disturbs the OF autopilot but the point of application of this disturbance differs from that of the relief disturbance (see Fig. 6a). A light headwind (produced by a fan) was observed to reduce the MH groundspeed (Fig. 10b, dotted curve). The reduction in speed forced the groundheight  $h$  to decrease in similar proportion (figure 10a). Since the speed increased again when the robot left the wind-swept region of the arena, the MH rose again. This MH flight pattern therefore accounts particularly well for the field data cited above. A strong head wind reduced the groundspeed so much that it forced the MH to land (Fig. 10a, continuous curve). Landing was smooth, however, because  $h$  was decreased under

*visually closed loop*, in proportion to  $V_x$ . This finding is highly reminiscent of what occurs in many insects and birds, which descend by headwind and settle when the wind grows stronger (Kennedy, 1939, 1951; Williams, 1965; Alestam, 1990). Given the natural decrease in wind speed that occurs close to the earth in the boundary layer, these reactions can be said to be “ecological” because they allow the insects to travel farther for the same amount of energy (this point is discussed extensively in Ruffier & Franceschini, 2005). What the explicit control scheme (Fig. 6) brings to the fore is the direction of causality: it is the change in groundspeed that induces the change in groundheight, and not the other way round (this point is discussed further in Section 8).

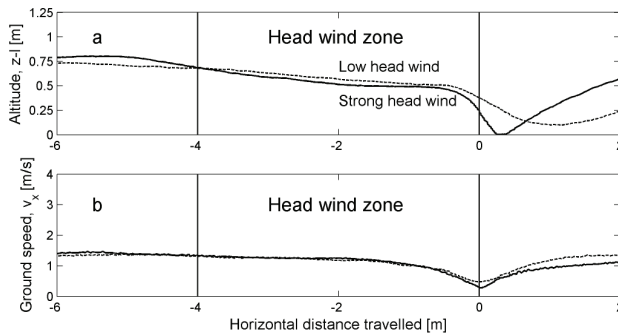


Figure 10. Reaction of the miniature helicopter (MH) to head wind (dashed curves: low head wind,  $V_w = 0.5\text{m/s}$ ; continuous curves: strong head wind,  $V_w = 1.5\text{m/s}$ ). The OCTAVE autopilot (Fig. 6a) makes the MH react to the reduction in speed (b) by reducing its altitude (a). The strong wind forced the MH to land at negligible forward speed (continuous curves). In these experiments, a  $30 \times 20\text{cm}$  planar airfoil was mounted perpendicular to the travel axis to catch the wind better, emphasizing the effect (From Ruffier & Franceschini, 2004)

#### 7.4 Flying over mirror-smooth water

Bees crossing mirror-smooth water during foraging trips were reported to fly lower and lower until crashing head-first into the water. They were rescued from drowning only when the water surface was rippled or when a slatted bridge was placed on the water surface to provide sufficient contrast (Heran & Lindauer, 1963). Recent studies on bees trained to fly across a lake did not quite confirm these early results (Tautz et al., 2004), but the (large) lake may not have been as ripple-free as the (small) flooded quarry used in the original experiments.

A featureless expanse of water no longer provides the animal’s eye with any contrasting features, and the OF sensor will no longer respond. If we make the feedback signal  $\omega_{meas} = 0$  in figure 6a, the error signal  $\epsilon$  becomes large and negative (equal to  $\omega_{set}$ ), which leads to a fatal decrease in groundheight  $h$ . The *OF regulator* therefore may account for the puzzling finding that bees plunge straight into calm water during their foraging trip. The closed feedback loop irrevocably pulls the insect down whenever the OF sensor fails to respond. A similarly disastrous tendency was observed in the MH when it was flying over a ground that was made deliberately blank over a distance of 1.5 meters. A simple way to rescue the MH flight from this dangerous situation consisted in holding the last OF measurement for some time (e.g., 0.5 seconds, see figure 9 in Ruffier & Franceschini, 2005).

## 7.5 Landing

Video recording of landing honeybees showed that their grazing landings on a flat surface occur with a constant slope (Srinivasan et al., 2000). Bees were assumed to meet two requirements to be able to land smoothly: "(i) adjusting the speed of forward flight to hold constant the angular velocity of the image of the surface as seen by the eye, (ii) making the speed of descent proportional to the forward speed"(Srinivasan et al., 2000). Our OF regulator scheme (Fig. 6a) controls not the forward flight speed but the vertical lift, and predicts that the bee should land with a constant slope, as actually observed in the MH flight pattern (Fig. 8a, right part).

Both MH's and bees' landing behavior can be explained in the same way because the surge dynamics can be described in both cases by similar (first order) linear differential equations (see Supplements in Franceschini & al., 2007).

Landing of the MH is initiated by commanding it to gradually pitch backwards to the vertical (at arrowhead 3 in figure 8a), which induces a gradual loss of speed (figure 8b). The groundheight  $h$  is then bound to decrease proportionally to  $V_x$  since the feedback loop strives to make  $V_x/h = \text{constant}$  (Eq. 2).

The *final approach* actually starts when the MH reaches the upright position (arrowhead 4 in Fig. 8a). From this moment onwards,  $V_x$  decreases exponentially with the "surge time constant"  $\tau_{MH} = 2.15\text{s}$  (see figure 4 in Franceschini & al., 2007) and the feedback loop forces  $h$  (and therefore its derivative  $dh/dt$ , i.e., the descent speed  $V_z$ ) to decrease with the same time constant. The descent speed:groundspeed ratio  $V_z(t):V_x(t)$ , that is, the descent *slope*, will therefore remain constant throughout the final approach, as actually observed in both landing bees (Srinivasan et al., 2000) and the landing MH (figure 8a).

In (Franceschini & al., 2007), we established that the ensuing descent angle  $\alpha$  [rad] can be calculated as follows :

$$\alpha = -\arctan\left(\frac{1}{\omega_{set}\tau}\right)$$

where  $\omega_{set}$  = OF set-point [ $\text{rad.s}^{-1}$ ], and  $\tau$  = surge time constant [s] of the MH ( $\tau_{MH} = 2.15\text{s}$ ).

This means that the slope of the final approach depends on only two parameters: the surge time constant and the OF set point.

If the constant-slope landing glide observed in bees reflects the presence of an *OF regulator* onboard these insects, then by substituting the landing data obtained on bees (Srinivasan et al., 2000):  $\alpha_{BEE} = -28^\circ$ ;  $\omega_{setBEE} = 500 \text{ deg.s}^{-1}$ , into Eq. 3, we can determine the bee's *surge time constant* :

$$\tau_{BEE} = 0.22\text{s}$$

It is striking that this value predicted by our *OF regulator* model matches closely the time constant values (0.22s, 0.27s, 0.29s and 0.57s) that we derived from the data of Srinivasan and coworkers (2000) on the exponential decrease in bees' *groundheight* with time. This makes the OF regulator scheme (Fig. 6a) an appealing hypothesis for the control system that is implemented onboard the bee.

## 8. A dual optic flow regulator for joint speed control and lateral obstacle avoidance

The model presented above differs from another one where the OF would control the groundspeed  $V_x$  rather than the groundheight  $h$  (Preiss & Kramer, 1984; Srinivasan et al., 1996, 2000; Baird et al., 2005). If the ventral OF controlled  $V_x$  instead of  $h$  in figure 6a, this would lead to strikingly different flight patterns from those observed in insects by previous authors, as follows:

(i) instead of following a slanting terrain, as migrating butterflies (Williams, 1965; Srygley & Oliveira, 2001) and our MH do, the insect would gradually decelerate until touching the rising ground at a negligible speed, thus inopportunistically interrupting its journey.

(ii) instead of descending in a headwind and rising in a tailwind, as occurs in honeybees (Braüniger, 1964), locusts (Kennedy, 1951), dung-beetles (Steiner, 1953), mosquitoes (Kennedy, 1939), and our MH (figure 10), the insect would compensate for the unfavourable headwind by increasing its airspeed without changing its groundheight.

These two models can be reconciled, however, if we add the hypothesis that another *OF regulator*, based on OF sensors from the *lateral* parts of the eyes, may be in charge of controlling the groundspeed  $V_x$ .

In line with the OCTAVE autopilot, we designed the LORA III autopilot (LORA III stands for Lateral Optic flow Regulator Autopilot, mark III), which is able to control both the forward speed  $V_x$  of an aerial vehicle and its lateral distances  $D_r$  and  $D_l$  to the two walls of a corridor (Fig. 11).

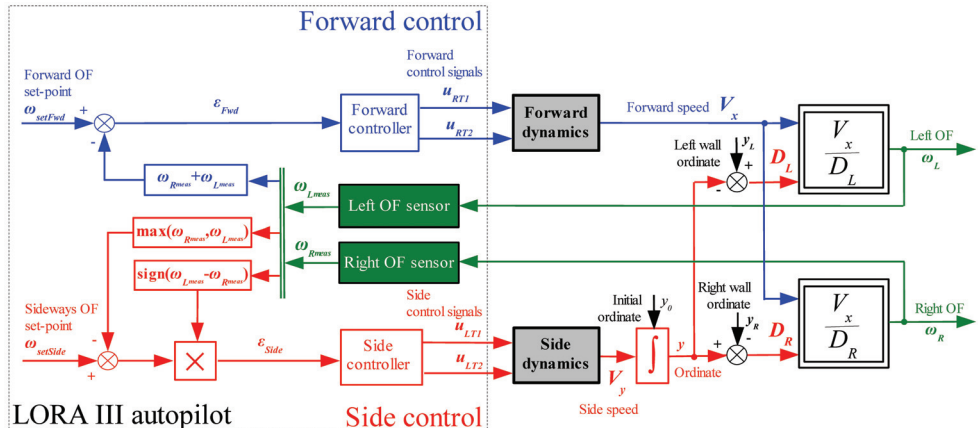


Figure 11. The LORA III autopilot is a *dual OF regulator* that enables a *fully actuated* hovercraft to navigate in a (straight or tapered) corridor by controlling its forward speed  $V_x$  and its distance  $D_r, D_l$  to the walls jointly, without requiring any speed or distance measurements (From Serres et al., 2008a)

We showed the feasibility of this scheme in simulation experiments where a miniature hovercraft navigates in a straight or tapered corridor (Serres et al., 2008a). Our hovercraft is equipped with two additional *lateral thrusters* that make it *fully actuated*. This means that it is capable of independent side-slip and forward slip, like hymenopteran insects (Zeil et al., 2008). The groundspeed is constrained by the environment, as observed on bees navigating in a

straight or tapered corridor (Srinivasan et al., 1996). The clearance to the walls is constrained by the environment as well, but the robot does not show a systematic “centering behavior”, in contrast with former observations on bees (Kirschner & Srinivasan, 1989). However, the robot’s “wall-following behavior” observed is fully consistent with the results of our own behavioural experiments on bees navigating in a large corridor (Serres et al. 2008b).

LORA III is based on only two OF sensors (one looking to the right, one to the left). The forward speed  $V_x$  is controlled by the error signal  $\epsilon_{Fwd}$  between the sum of the two OFs (right and left) and the forward OF set point  $\omega_{setFwd}$ . The lateral distance to the walls is controlled by the error signal  $\epsilon_{Side}$  between the larger of the two OFs and the sideways OF set point  $\omega_{setSide}$ . The LORA III *dual OF regulator* accounts particularly well for both types of behaviours. The typical “wall-following behavior” that we observed on both the bees and the robot can be shown to degenerate into a “centering behavior” for particular *relative* values between the two OF set points  $\omega_{setFwd}$  and  $\omega_{setSide}$  (Serres et al., 2008a, Serres, 2008). The advantage of this control scheme is that it determines both the forward speed and the distance from the walls on the sole basis of two parameters - two OF set points - without any needs for measuring forward speed, lateral distances and corridor width, that is, without using any velocimeters or range finders. Extensive simulation experiments in straight or tapered corridors were presented in (Serres et al., 2008).

## 9. OSCAR as a yaw control autopilot

Electrophysiological recordings on freely flying flies have revealed that the muscle attached to the base of the retina (Burtt & Patterson, 1970; Hengstenberg, 1971) causes *retinal microscanning*: the whole retinal mosaic (Fig.1a) translates repeatedly at about 5 Hz by a few micrometers underneath the facet mosaic, causing the visual axes to *rotate* by a few degrees (Franceschini & Chagneux, 1997). Such a purely *rotational OF* is exploited on-board another aerial robot we built: robot OSCAR (Fig. 12a).

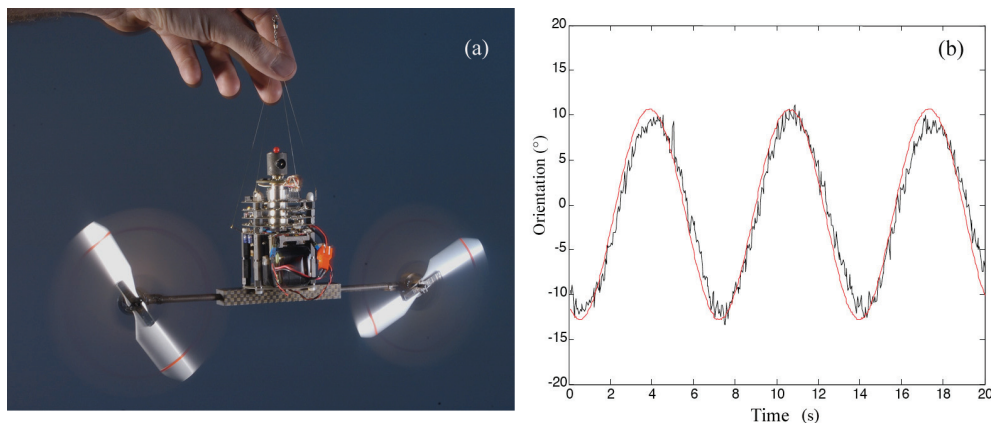


Figure 12. (a) OSCAR is a 100-gram twin-engine robotic demonstrator that sees. It is equipped with an elementary eye (visible on top), composed of a lens and only two photoreceptors driving an EMD of the type shown in Fig. 3 (Photo by H. Raguet) (b) Smooth pursuit (tracking) of a dark edge (contrast  $m = 0.4$ ) displaced sinusoidally at 0.15 Hz in a frontal plane situated 1.3 meters from the eye (From Viollet & Franceschini, 1999b)

This project was based on the assumption that microscanning in flies operates in connection with motion detection. On the basis of this fly's retinal microscanning process, we developed an optronic sensor (Viollet & Franceschini, 1999a), and a novel aerial robot, equipped with this sensor (Viollet & Franceschini, 1999b, 2001). OSCAR is attached to a thin, 2-meter long wire secured to the ceiling of the laboratory. It is free to adjust its yaw by driving its two propellers differentially, and it does so in spite of the many (aerodynamic or pendular) disturbances it encounters.

Thanks to its microscanning eye, this miniature (100-gram) robot is not only able to fixate a nearby "target" (a dark edge or a bar) steadily but also to track it at angular speeds of up to 30°/s - a value similar to the maximum tracking speed of the human eye. It cannot, however, estimate the distance from the target since it deals only with the *rotational OF*.

The OSCAR sensor is able to *detect* a bar subtending an angle much smaller than the interreceptor angle  $\Delta\phi = 4^\circ$ , making it applicable for nonemissive power line detection on-board fullscale helicopters (Viollet et al., 2006). The OSCAR sensor is also able to *locate* an edge with great positioning accuracy (0.1 degrees, which is 40 times smaller than  $\Delta\phi$ ): OSCAR has acquired *hyperacuity* (Viollet & Franceschini, 2001). This property makes the principle appealing for accurate stabilization of various platforms (Franceschini et al., 2005). Inspired by the fly's thoracic halteres that have long been known to act as gyroscopes, we equipped the OSCAR robot with an additional inertial feedback based on a MEMS *rate gyro*. The interplay of the two (visual and inertial) control loops enhances both the dynamic stability and performances of the fixation and tracking system (Viollet & Franceschini, 1999b, 2001). More recently, we introduced a mechanical *decoupling* between eye and body, and implemented a genuine *vestibulo-ocular reflex* that was key to maintaining the robot's gaze perfectly fixed on the target (Viollet & Franceschini, 2005, Kerhuel et al., 2007). Robot OSCAR II is a novel 100-gram aerial robot whose gaze, decoupled from the heading, remains robustly locked onto a target in spite of various perturbations that we deliberately applied to the body. It is the gaze orientation of OSCAR II that ultimately controls its heading (Viollet et al., this volume).

## 10. Summary and conclusion

In this chapter, we reported about our attempts to understand *how* flying insects could behave on the basis of OF cues. We presented several bio-inspired, OF based visual guidance principles and showed that they may be helpful in the context of autonomous guidance of MAVs over a terrain or in a corridor. The principles we came up with differ markedly from a current OF based navigation strategy. The latter requires that OF sensors be associated with a groundspeed sensor (based on GPS, for example) in order to determine the groundheight (see Eq 1) to achieve terrain following or landing (Barrows et al., 2003; Barber et al., 2005; Srinivasan et al., 2006; Garrat & Chahl, 2008).

OCTAVE and LORA III autopilots harness the power of the *translational OF* in a quite different manner. They do not need to estimate any speed or range, and they do not aim to achieve any "speed holding" or "range holding" abilities. They aim instead at producing safe behavior by a process that can be called "OF hold". These autopilots consist of feedback control loops, called « *optic flow regulators* ». Their block diagrams (Figures 6 & 11) pinpoint which variables are to be *measured* or *controlled* or *regulated*, and give the *causal* and *dynamical* relationships between these variables. Three (ventral, forward and sideways) *OF regulators*

strive to maintain a given OF  $\omega$  constant by acting upon the lift, the forward thrust or the side thrust, respectively. OF sensors are shown to be sufficient for these tasks and there is no need to measure (or estimate) groundspeed, groundheight and clearance to the walls in a corridor. Simulation experiments and robotic demonstrators showed that risky maneuvers such as automatic takeoff, ground avoidance, level flight, terrain following, landing, centering, wall following, and groundspeed control can all be successfully performed on the basis of these three *OF regulators*. Moreover, these control schemes were found to account for a series of puzzling, seemingly unconnected flying abilities observed by many authors over the last 70 years in numerous insect species, suggesting that *OF regulators* may well be implemented onboard insects (see Sections 7 & 8).

Three parameters - the three OF set-points  $\omega_{set}$  of Fig. 6 and 10 - would suffice to determine the flight behavior, at least in the simplified, random but richly contrasted environments considered here. Onboard the insect, these set-points may depend on either innate, internal or external factors.

Electronic implementation of an *OF regulator* is not very demanding - nor is its neural implementation - since it relies upon a few linear operations (such as summation, difference and various filters) and nonlinear operations (such as minimum or maximum detection). The worthiest component of an OF regulator is the OF sensor itself. Like the honeybee's Velocity Tuned (VT) neurons (Ibbotson, 2001), the neuromorphic OF sensors we have been building since 1985 deliver an output that grows monotonically with the OF  $\omega$ , with little dependence on spatial frequency and contrast (see Section 3). Their respond over a 10-fold range in OF (from 40°/s to 400°/s: Ruffier et al., 2003; Aubépart & Franceschini, 2007). This range is largely sufficient because each OF sensor needs only to detect a *deviation*  $\epsilon$  from the OF set point. The miniature helicopter flight pattern illustrates this point: the ventral *OF regulator* produces a behavior such that the OF output  $\omega_{meas}$  varies little throughout the journey, from takeoff to landing (Fig. 8c). A similar observation holds for the OF sensors of the forward and sideways *OF regulators* (see Figs 7c,e & 12c,e in Serres et al., 2008a).

Each OF sensor at work on our proof of concept robots is characterized by a low resolution. The inter-receptor angle in the eyes of OCTAVE, LORA III and OSCAR robots is around 4°, a value close to the interommatidial angle (5°) of the fruitfly's eye (Franceschini, 1975). The field of view (FOV) of the eyes and the provocatively small number of pixels (2 pixels per ventral or lateral eye) will obviously need to be increased. Covering the frontal part of the FOV, in particular, will be essential to sense and avoid obstacles directly in the flight path, and here the retinal microscanning principles could be a great help (Mura & Franceschini, 1996; Viollet & Franceschini, 2001). A recent study showed that a more frontally oriented EMD may provide OCTAVE autopilot with a feedforward anticipatory signal that helps the robot climb steeper rises (Ruffier & Franceschini, 2008).

The control schemes we proposed are simple but thus far limited to the use of the maximal OF sensed either ventrally or laterally, perpendicular to the heading direction. Once developed beyond the state of the current minimalistic robotic demonstrators, OCTAVE and LORA III principles could potentially be harnessed to guide a MAV indoors or through complex terrains such as mountainous canyons or urban environments. Since the control systems are parsimonious and do not rely on GPS or any emissive (power-hungry) sensors such as RADARs or LADARs, they promise to match the draconian constraints imposed upon micro aerial vehicles, in terms of size, mass and consumption.

For the same reasons, these autopilots could potentially be developed for robotic missions on other planets or moons. A Martian rover could make use of the OCTAVE principle, since it ensures safe automatic landing (see Section 7.5). A rover flying in Martian canyons and gullies could make use of the LORA III principle, since both the craft's groundspeed and its clearance to the walls would automatically depend on the canyon's width (see Section 8, and Serres et al, 2008a). Whether on Earth or on another celestial body, the craft would need to receive from the earth based (or orbital) station only three *low bandpass* signals: the OF set-points.

## 11. Acknowledgments

We are grateful to F. Aubépart L. Kerhuel and G. Portelli for their fruitful comments and suggestions during this research. We are also grateful to Marc Boyron (electronics engineer), Yannick Luperini and Fabien Paganucci (mechanical engineers) for their expert technical assistance. Serge Dini (beekeeper) gave plenty of advices during the behavioral experiments. This research was supported by CNRS (Life Science ; Information and Engineering Science and Technology), by an EU contract (IST/FET-1999-29043) and a DGA contract (2005-0451037).

## 12. References

- Alestam, T. (1990). *Bird Migration*. Cambridge University Press
- Aubépart, F. & N. Franceschini., N. (2007). Bio-inspired optic flow sensors based on FPGA: application to micro-air vehicles. *Journal Microprocessors and Microsystems* 31, 408-419
- Aubépart, F., El Farji, M. & Franceschini, N. (2004). FPGA implementation of elementary motion detectors for the visual guidance of micro-air vehicles. *Proceedings of IEEE International Symposium on Industrial Electronics (ISIE'2004)*, Ajaccio, France, pp. 71-76
- Aubépart, F., Serres, J., Dilly, A., Ruffier, F. & Franceschini., N. (2008). Field programmable gate arrays (FPGA) for bio-inspired visuo-motor control systems applied to micro-air vehicles, In: *Aerial Vehicles*, published by In-Tech
- Baird, E., Srinivasan, M.V., Zhang, S.W. & Cowling, A. (2005). Visual control of flight speed in honeybees. *Journal of Experimental Biology* 208, 3895-3905
- Baird, E., Srinivasan, M.V., Zhang, S.W., Lamont R. & Cowling, A. (2006).Visual control of flight speed and height in the honeybee. In: *From Animals to Animats 9*, S. Nolfi et al. (Eds.), 4095, 40-51
- Barber, D.B.; Griffiths, S.R.; McLain, T.W.;& Beard, R.W. (2005) Autonomous landing of miniature aerial vehicles. In: *Proceedings of American Institute of Aeronautics and Astronautics Conference*
- Barrows, GL, Neely, C. & Miller, K.T. (2001). Optic flow sensors for MAV navigation. In : Fixed and flapping wing aerodynamics for micro-air vehicle applications. *Progress in Astronautics and Aeronautics*, Vol. 195, 557-574
- Barrows, GL; Chahl, J.S.; Srinivasan MV. (2003) Biologically inspired visual sensing and flight control. *Aeronautic Journal* 107, 159-168

- Blanès, C. (1986) Appareil visuel élémentaire pour la navigation à vue d'un robot mobile autonome. *MS thesis in Neuroscience*, University of Aix-Marseille II, Marseille, France
- Blanès, C. (1991). Guidage visuel d'un robot mobile autonome d'inspiration bionique. *PhD thesis*, Polytechnical Institute, Grenoble, France (thesis work at the Neurocybernetics lab, CNRS, Marseille, France)
- Borst, A. & Haag, J. (2002). Neural networks in the cockpit of the fly. *Journal of Comparative Physiology A* 188, 419-437
- Braitenberg, V. (1967). Patterns of projection in the visual system of the fly, I/Retina-Lamina projections. *Experimental Brain Research* 3, 271-298
- Bräuninger, H.D. (1964). Über den Einfluss meteorologischer Faktoren auf die Entfernungsweisung im Tanz der Bienen. *Zeitschrift für Vergleichende Physiologie* 48, 1-130
- Buchner E. (1984). Behavioral analysis of spatial vision in insects In: *Photoreception and Vision in Invertebrates*, Ali, M. (Ed.), New-York : Plenum, 561-621
- Burtt, J. & Patterson, J. (1970). Internal muscle in the eye of an insect. *Nature* 228, 183-184
- David, C. (1978). The relationship between body angle and flight speed in free-flying Drosophila. *Physiological Entomology* 3, 191-195
- David, C. (1982). Compensation for height in the control of groundspeed by Drosophila in a new 'barber's pole' wind tunnel. *Journal of Comparative Physiology A* 147, 1432-1351
- Egelhaaf, M. & Borst, A. (1993). Movement detection in Arthropods. In : *Visual motion an its role in the stabilization of gaze*, F. Miles & J. Wallman, Eds., Amsterdam: Elsevier, 53-77
- Franceschini N. (1975). Sampling of the visual environment by the compound eye of the fly: fundamentals and applications, in: *Photoreceptor Optics*, A. Snyder, R. Menzel (Eds), Berlin : Springer, Chapt. 17, 98-125
- Franceschini, N. (1984). Chromatic organisation and sexual dimorphism of the fly retinal mosaic. In: *Photoreceptors*. Borsellino, A. and Cervetto, L. (Eds.), pp. 319-350
- Franceschini, N. (1985). Early processing of colour and motion in a mosaic visual system. *Neuroscience Research*, Supplement 2, 517-549
- Franceschini, N. (1992). Sequence-discriminating neural network in the eye of the fly. In: *Analysis and Modeling of Neural Systems*, F.H.K. Eeckman (Ed.), Norwell, USA, Kluwer Acad. Pub., 142-150.
- Franceschini, N. (2007). Sa majesté des mouches. In: *Voir l'Invisible*, JP.Gex (Ed.), Paris: Omnisciences (2007), pp 28-29
- Franceschini, N. (2008). Towards automatic visual guidance of aerospace vehicles: from insects to robots. *Acta Futura : Proceedings of the ESA International Symposium on Advanced Concepts : « A Bridge to Space »* Noordwick, (in press)
- Franceschini, N. & Chagneux, R. (1997). Repetitive scanning in the fly compound eye. *Proceedings of the 25th Göttingen Neurobiology Conference* (N. Elsner, H. Wässle, Eds.) Stuttgart, : G. Thieme, 279
- Franceschini, N., Blanes, C. & L. Oufar, L. (1986). Appareil de mesure, passif et sans contact, de la vitesse d'un objet quelconque. *Technical Report ANVAR/DVAR*, N°51549, Paris.
- Franceschini, N., Pichon, J.M. & Blanès, C. (1992). From insect vision to robot vision. *Philosophical Transactions of the Royal Society London B* 337, 283-294

- Franceschini, N., Kirschfeld, K., Minke, B. (1981a). Fluorescence of photoreceptor cells observed in vivo. *Science* 213, 1264-1267
- Franceschini, N., Hardie, Ribi, W., Kirschfeld, K. (1981b). Sexual dimorphism in a photoreceptor. *Nature* 291, 241-244
- Franceschini, N., Riehle, A. & Le Nestour A. (1989). Directionally selective motion detection by insect neurons. In: *Facets of Vision*, D.G. Stavenga and R.C. Hardie (Eds.), Berlin, Springer, 360-390.
- Franceschini, N., Ruffier, F. & Serres, J. (2007). A bio-inspired flying robot sheds light on insect piloting abilities. *Current Biology* 17, 329-335
- Franceschini, N.; Viollet, S. & Boyron, M. (2005). Method and device for hyperacute detection of an essentially rectilinear contrast edge, and system for fine following and fixing of said contrast edge. *International Patent PCT/FR2005/11536*
- Franceschini, N., Ruffier, F., Viollet, S. & Boyron, M. (2003). Steering aid system for altitude and horizontal speed, perpendicular to the vertical, of an aircraft and aircraft equipped therewith. *International Patent PCT/FR2003/002611*
- Garratt M.A. & Chahl, J.S. (2008). Vision-based terrain following for an unmanned rotorcraft. *Journal of Field Robotics* 25, 284-301
- Gibson, J.J. (1950). *The perception of the visual world*, Boston: Houghton Mifflin
- Gibson J.J., Olum, P. & Rosenblatt, F. (1955). Parallax and perspective during aircraft landings. *American Journal of Psychology* 68, 372-395
- Green, WF, Oh, Y. & Barrows, G. (2004). Flying insect inspired vision for autonomous axial robot maneuvers in near earth environments. *Proceedings of the IEEE International Conference on Robotics and Automation (ICRA04)* 2343-2352
- Hardie R.C. (1985). Functional organization of the fly retina. *Progress in Sensory Physiology* 5, Ottosson D. (Ed.), Springer, Berlin
- Hassenstein, B. & Reichardt, W. (1956) Systemtheoretische Analyse der Zeitreihenfolgen und Vorzeichenauswertung bei der Bewegungsperzeption des Rüsszelkäfers Chlorophanus. *Zeitschrift für Naturforschung* 11b, 513-524
- House, K. (1993). Decoding of retinal image flow in insects. In : *Visual motion an its role in the stabilization of gaze*, F.A. Miles and J. Wallman (Eds.) Amsterdam : Elsevier, 203-235
- House, K. & Egelhaaf, M. (1989) Neural mechanisms of course control in insects. In: *Facets of vision*; D.G. Stavenga & R.. Hardie, Berlin, Springer pp. 391-424
- Hengstenberg, R. (1971). Das Augenmuskel System der Stubenfliege Musca domestica. *Kybernetik* 2 56-77
- Heran, H. (1955). Versuche über die Windkompensation der Bienen. *Naturwissenschaften* 5, 132-133
- Heran, P. & Lindauer, M. (1963). Windkompensation und Seitenwindkorrektur der Bienen Flug über Wasser. *Zeitschrift für vergleichende Physiologie* 47, 39-55
- Heisenberg, M, Wolf ,R. (1984). *Vision in Drosophila*. Berlin, Springer.
- Ibbotson, M.R. (2001). Evidence for velocity-tuned motion-sensitive descending neurons in the honeybee. *Proceedings of the Royal Society, London B* 268, 2195-2201
- Kennedy, J.S. (1939). Visual responses of flying mosquitoes. *Proceedings of the Zoological Society of London* 109, 221-242
- Kennedy, J.S. (1951). The migration of the desert locust (*Schistocerca gregaria* Forsk.) I. The behaviour of swarms. *Phil. Transactions of the Royal Society, London, B* 235, 163-290

- Kerhuel, L., Viollet, S. & Franceschini, N. (2007). A sighted aerial robot with fast gaze and heading stabilization. *Proceedings of the IEEE International Conference on Intelligent Robots and Systems (IROS)*, San Diego, USA, pp. 2634-2641
- Kirchner, W.H. & Srinivasan, M.V. (1989). Freely moving honeybees use image motion to estimate distance. *Naturwissenschaften* 76, 281-282
- Kirschfeld, K. (1967). Die Projektion der optischen Umwelt auf das Raster der Rhabdomere im Komplexauge von Musca. *Experimental Brain Research* 3, 248-270
- Kirschfeld, K.; Franceschini, N. (1968). Optische Eigenschaften der Ommatidien im Komplexauge von Musca. *Kybernetik* 5 47-52
- Kirschfeld, K.; Franceschini, N., Minke, B. (1977). Evidence for a sensitizing pigment in fly photoreceptors » *Nature* 269, 386-390
- Koenderink, J.J. (1986). Optic flow. *Vision Research* 26, pp. 161-79
- Kramer, J., Sarapeshkar, R. & Koch C. (1995). An analog VLSI velocity sensor. In *Proceedings of IEEE International Symposium on Circuits and Systems, Seattle*, USA, pp 413-416
- Krapp, H, Hengstenberg, B, Hengstenberg, R.(1998). Dendritic structure and receptive-field organisation of optic flow processing interneurons in the fly, *Journal of Neurophysiology* 79, 1902-1917.
- Laughlin, S. (1984). The role of parallel channels in early visual processing by the arthropod compound eye. In: *Photoreception and vision in invertebrates*. M.A. Ali Ed., Plenum, 457-481
- Lee, D. N. (1980). The optic flow field: the foundation of vision. *Philosophical Transactions of the Royal Society London B* 290, 169-179
- Marr, D. (1982). *Vision*, San Francisco: Freeman
- Moeckel, R. & Liu S.C. (2007). Motion detection circuits for a time-to-travel algorithm. *Proceedings IEEE Int. Symposium Circuits and Systems (ISCAS07)*, pp. 3079-3082
- Mura, F. & Franceschini., N. (1994). Visual control of altitude and speed in a flying agent. In : *From Animals to Animats III*, D. Cliff et al. (Eds), Cambridge: MIT Press, 91-99
- Mura, F.; Franceschini, N. (1996). Obstacle-avoidance in a terrestrial mobile robot provided with a scanning retina. *Proceedings IEEE International Symposium on Intelligent Vehicles*. N. Aoki and I. Masaki, eds., Seikei University, Tokyo, Japan, pp. 47-52.
- Netter, T. & Franceschini, N. (1999). Neuromorphic optical flow sensing for nap-of-the-Earth flight. In : *Mobile Robots XIV*, D. Gage and H. Choset (Eds), SPIE, Vol. 3838, 208-216
- Netter, T. & Franceschini, N. (2002). A robotic aircraft that follows terrain using a neuromorphic eye. In : *Proceedings of the IEEE International Conference on Intelligent Robots and Systems (IROS)* Lausanne, Switzerland, pp. 129-134
- Pichon, J-M., Blanès, C. & Franceschini, N. (1989). Visual guidance of a mobile robot equipped with a network of self-motion sensors. In : *Mobile Robots IV*, W.J. Wolfe , W.H. Chun (Eds.) Bellingham, U.S.A : SPIE , Vol. 1195, 44-53
- Portelli, G., Serres, J., Ruffier F. & Franceschini, N. (2008). An Insect-Inspired Visual Autopilot for Corridor-Following. *Proceedings of the 2<sup>nd</sup> Biennial IEEE Int. Conference on Biomedical Robotics and Biomechatronics*, BioRob 08, Scottsdale, USA, pp. 19-26
- Preiss, R. (1992). Set point of retinal velocity of ground images in the control of swarming flight of desert locusts. *Journal Comparative Physiology A* 171, 251-256
- Preiss, R. & Kramer, E. (1984). Control of flight speed by minimization of the apparent ground pattern movement. In: *Localization and Orientation in Biology and Engineering*, D. Varju and H. Schnitzler, eds. (Berlin, Springer), 140-142

- Pudas, M. ; Viollet, S. ; Ruffier, F. ; Kruusing, A. ; Amic, S. ; Leppävuori, S. & Franceschini, N. (2007). A miniature bio-inspired optic flow sensor based on low temperature co-fired ceramics (LTCC) technology, *Sensors and Actuators A* 133, 88-95
- Reichardt, W. (1969): Movement perception in insects. In: *Processing of Optical Data by Organisms and by Machines*, W. Reichardt (Ed.), New York: Academic Press , 465-493
- Riehle, A. & Franceschini, N. (1984). Motion detection in flies: parametric control over ON-OFF pathways. *Experimental Brain Research* 54, 390-394
- Ruffier, F. & Franceschini, N. (2003) OCTAVE, a bioinspired visuo-motor control system for the guidance of Micro-Air Vehicles, In: *Bioengineered and Bioinspired Systems*, A. Rodriguez-Vazquez et al., Eds., Bellingham, U.S.A , SPIE, Vol. 5119, 1-12
- Ruffier, F. & Franceschini, N. (2004a). Visually guided micro-aerial vehicle: automatic take-off, terrain following, landing and wind reaction. *Proceedings IEEE International Conference on Robotics and Automation (ICRA04)*, New Orleans, USA, pp. 2339-2346
- Ruffier, F. & Franceschini, N. (2004b). Optic flow based AFCS for rotorcraft automatic maneuvering (terrain following, takeoff and landing). *Proceedings of the 30th European Rotorcraft Forum*, AAF/CEAS, Marseille, 71.1-71.9.
- Ruffier, F. & Franceschini, N. (2005). Optic flow regulation: the key to aircraft automatic guidance. *Robotics and Autonomous Systems* 50, 177-194
- Ruffier, F. & Franceschini, N. (2008). Aerial robot piloted in steep relief by optic flow sensors. *Proceedings of the IEEE/RSJ International Conference on Intelligent Robots and Systems (IROS08)*, Nice, France, pp. 1266-1271.
- Ruffier, F.; Viollet, S.; Amic, S. & Franceschini, N. (2003). Bio-inspired optical flow circuits for the visual guidance of micro-air vehicles. *Proceedings the IEEE International Symposium on Circuits and Systems (ISCAS)*, Bangkok, Thailand, III, pp. 846-849
- Serres, J. (2008). De l'abeille au robot : la « régulation du flux optique », *PhD Thesis*, University of Montpellier, France (Thesis work from the Biorobotics lab, CNRS, Marseille, France).
- Serres, J.; Dray, D.; Ruffier, F. & Franceschini, N. (2008a). A vision-based autopilot for a miniature air vehicle: joint speed control and lateral obstacle avoidance. *Autonomous Robots* 25, 103-122
- Serres, J.; Masson, G.; Ruffier, F. & Franceschini, N. (2008b). A bee in the corridor : centring and wall following. *Naturwissenschaften*, 95 (12) 1181-1187
- Shoemaker, P.A. ; O'Caroll, D.C. & Straw, A.D. (2005). Velocity constancy and models for wide-field visual motion detection in insects. *Biological Cybernetics*, 93, 275-287
- Srinivasan, M.V. (1993). How insects infer range from visual motion. In : *Visual motion and its role in the stabilization of gaze*. F.A. Miles and J. Wallman, Eds. Amsterdam : Elsevier, 139-156
- Srinivasan, M.; Thurrowgood, S. & Soccol, D. (2006). An optical system for guidance of terrain following in UAVs. *Proceedings of the IEEE International Conference on video and signal based surveillance AVSS06*
- Srinivasan, M.V.; Lehrer, M.; Kirchner, W.H. & Zhang, S.W. (1991). Range perception through apparent image speed in freely flying honeybees. *Visual Neuroscience* 6, 519-535
- Srinivasan, M.V., Zhang, S.W. and Chandrashekara K. (1993). Evidence for two distinct movement-detecting mechanisms in insect vision. *Naturwissenschaften* 80, 38-41.

- Srinivasan, M.V., Zhang, S.W., Lehrer, M. & Collett., T. (1996). Honeybee navigation en route to the goal: visual flight control and odometry. *Journal of Experimental Biology*, 199, 237-244
- Srinivasan, M.V., Zhang, S.W., Chahl, J.S., Barth, E. & Venkatesh, S. (2000). How honeybees make grazing landings on flat surface. *Biological Cybernetics* 83, 171-183
- Srygley, R.B. & Oliveira, E.G (2001). Orientation mechanisms and migration strategies within the flight boundary layer. *Insect movements: mechanisms and consequences*. T.P. Woiwod, D.R. Reynolds and C.D. Thomas (Eds.), CAB international, 183-206
- Steiner, G. (1953). Zur Duftorientierung fliegender Insekten. *Naturwissenschaften* 19, 514-515
- Straw AD, Rainsford T. & O'Carroll DC. (2008). Contrast sensitivity of insect motion detectors to natural images. *Journal of Vision* 8, 1-9
- Tautz, J., Zhang, S., Spaethe J., Brockman A., Si, A. & Srinivasan M.V. (2004). Honeybee odometry: Performance in varying natural terrain. *PLOS Biology*, 2, 915-923
- Taylor G.K. & Krapp, H.G. (2008). Sensory systems and flight stability : what do insects measure and why ? In : *Advances in Insect Physiol. 34 : Insects mechanisms and control*, J. Casas and S.J. Simpson (Eds.) Amsterdam : Elsevier, 231-316
- Ullman, S. (1981). Analysis of visual motion by biological and computer systems, *Computer* 14, 57-69
- Viollet, S. & Franceschini, N. (1999). Biologically-Inspired Visual Scanning Sensor for Stabilization and Tracking . *Proceedings of the IEEE International Conference on Intelligent Robots and Systems* (IROS 99) Kyon-gyu, Corea, pp. 204-209
- Viollet, S. & Franceschini, N. (1999). Visual servo system based on a biologically-inspired scanning sensor. *Proceedings of the Conference on sensor fusion and decentralized control in robotics II*, Bellingham, U.S.A : SPIE Vol. 3839, 144-155
- Viollet, S. & Franceschini, N. (2001). Super-Accurate Visual Control of an Aerial Minirobot In : *Autonomous minirobots for Research and Edutainment*, U. Rückert, J. Sitte, U. Witkowski (Eds.), Heinz Nixdorf Institut, Paderborn, Germany, 215-224
- Viollet, S. & Michelis, J. & Franceschini, N. (2006). Toward a bio-inspired nonemissive powerline detection system. *Proceedings of the 32th European Rotorcraft Forum*, ERF06, Maastricht, Netherlands, Paper N° AD09
- Viollet, S. & Franceschini, N. (2005). A high speed gaze control system based on the Vestibulo-Ocular Reflex. *Robotics and Autonomous Systems* 50 147-161
- Viollet, S., Kerhuel, L. & Franceschini, N. (2008). A novel biomimetic steering control system for sighted vehicles. In : *Intelligent Aerial Vehicles*, In: Aerial Vehicles, published by In-Tech
- Whiteside, T.C. & Samuel, G.D. (1970). Blur zone. *Nature* 225, 94-95
- Williams, C.P. (1965). *Insect migration*. London: Collins, second edition
- Zeil, J., Boeddeker, N. & Hemmi, J.M. (2008). Vision and the organization of behavior, *Current Biology* 18, 320-323